From bowls to capsules: assembly of hexanuclear Ni^{II} rings tailored by alkali cations.

Júlia Mayans,[a] Constantinos C. Stoumpos,[b] Mercé Font-Bardia[c] and Albert Escuer*[d]

Abstract: An anionic hexanuclear Ni^{II} metallamacrocycle with *endo* and *exo* linking sites has been employed as a building block to generate ~~a~~ series of capsules and bowls of nanometric size. The supramolecular arrangement of the $\{Ni_6\}$ rings was tailored by the size of the alkali cations~~,~~ showing the transition from $\{Ni_6\text{-}M_2\text{-}Ni_6\}$ capsules (M = Li^I and Na^I) to $\{Ni_6\text{-}M\}$ bowls (M = K^I and Cs^I). The alkyl co-cations are determinant to stabilize the assemblies by means of CH···π interactions on the *exo* side of the metallamacrocycles. The effect on the topology of the supramolecular assemblies of the cation size, cation charge, Et_3NH^+ or Me_4N^+ countercations has been analysed. Magnetic mesurements reveal the presence of ferromagnetic and antiferromagnetic interactions inside the rings that allow a $S = 0$ ground state.

Introduction

Supramolecular entities having cavities able to encapsulate guest molecules have been widely studied along the last years in several research fields such catalysis,[1] sensing and recognition[2-4] or biological mimics[5,6] profiting that the properties or conditions inside the cavities are different of the bulk solution and can promote specific reactivity. Systems of this kind have been often obtained by the employment of robust preformed organic receptors (calixarenes, cyclodrextrines, etc.) able to generate bowls or capsules by means of weak host-guest interactions.[7] Metallacages, based on coordination chemistry tools, have been obtained by the self-assembly of cations and organic linkers and usually anionic encapsulation is observed profiting its cationic character.[8,9] A recent advance in this field consist of the multi-guest systems built from heterotopic hosts exhibiting *endo-exo* linking sites that, in the best of the cases, can promote allosteric effects.[10]

Dipyridylketone (dpk) is an extensively studied reagent which in the presence of metal cation suffers an addition to its carbonyl group of water, methanol or acetonitrile promoting a variety of ligands $py_2CO(OH)^-$, $py_2C(MeO)O^-$ and $py_2C(CH_2CN)O^-$, respectively.[11] The system dpk/azide/Ni^{II} has yielded series of clusters[12-20] with nuclearities ranging from Ni_4 to Ni_9. Interestingly, in the presence of carbonato templating anion is prone to produce hexanuclear metallamacrocycles.[21,22] One of these systems, reported by Tong et al.,[22] is an anionic ring with formula $[Ni_6(\mu_6\text{-}CO_3)(N_3)_6(OAc)_3(py_2C(CH_2CN)(O))_3]^{2-}$ that was able to link potassium cations in a $\{Ni_{12}K_2\}$ cluster. Remarkably, this metallacycle was selectively obtained in the presence of potassium cations and without this cation the conventional defective cubane tetranuclear complex was stabilized.

In basis of the bibliographic data, we have explored the dpk/azide/Ni^{II} systems in basic media and at open air to favor the fixation of atmospheric CO_2 in non-carboxylate chemistry. Pyrazole (HPz) was employed to substitute the carboxylates, maintaining the charge balance of the anionic ring and its reactivity in the presence of different countercations. Following this strategy, series of capsules containing the $py_2C(O)(OH)^-$ ligand, Scheme 1, with formula $\{(Et_3NH)M(H_2O) \subset [Ni_6(CO_3)(N_3)_6(Pz)_3(py_2C(O)(OH))_3]\}_2$ were obtained for the smaller alkali cations M = Li^I (**1**) or Na^I (**2**) whereas the $(Et_3NH)M(H_2O) \subset [Ni_6(CO_3)(N_3)_6(Pz)_3(py_2C(O)(OH))_3]$ bowls were obtained for the larger alkali cations M = K^I (**3**) or Cs^I (**4**). Complex **1** was previously advanced as a communication.[23]

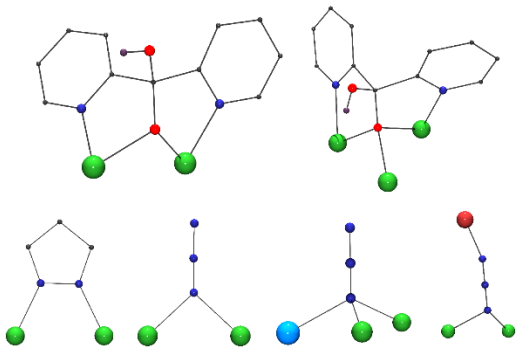

Scheme 1. Coordination modes for the $py_2C(O)(OH)^-$, azido and pyrazole ligands involved in compounds **1**-**6**. Color key: O, red; N, navy; Ni, green,

The border between the $\{Ni_{12}M_2\}$ and $\{Ni_6M\}$ nuclearities and the possible selectivity of the system was clarified in the 1:1 mixture of Na^I and K^I in the reaction media that yielded the co-

[a] Dr. J. Mayans
Instituto de Ciencia Molecular (ICMol), Universidad de Valencia, José Beltran 2, 46980 Paterna (Valencia), Spain.
[b] Dr. C. C. Stoumpos
Department of Materials Science and Technology
University of Crete
P. O. Box 2208, GR-71003, Heraklion, Greece
[c] Dr. M. Font-Bardia
Departament de Mineralogia, Cristal·lografia i Dipòsits Minerals and Unitat de Difracció de R-X. Centre Científic i Tecnològic (CCiTUB)
Universitat de Barcelona
Martí Franqués s/n, Barcelona-08028, Spain
[d] Prof. A. Escuer
Departament de Química Inorgànica i Orgànica, Secció Inorgànica and Institut de Nanociència i Nanotecnologia (IN^2UB).
Universitat de Barcelona
Martí i Franques 1-11, Barcelona-08028, Spain
E-mail: albert.escuer@qi.ub.es
www.ub.edu/inorgani/recerca/MagMol/magmol.htm

Supporting information for this article is given via a link at the end of the document.

crystallization of $\{(Et_3NH)M(H_2O) \subset [Ni_6(CO_3)(N_3)_6(Pz)_3(py_2C(O)(OH))_3]\}_2$ capsules (M = Na^I and K^I) (**5**). The organic countercation also show a key role in the stabilization of the rings as was evidenced by the chain of bowls obtained in the presence of Me_4N^+ with formula $\{(Me_4N)K(H_2O) \subset [Ni_6(CO_3)(N_3)_6(Pz)_3(py_2C(O)(OH))_3]\}_n$ (**6**) or the destabilization of the ring in the presence of sodium methoxide that yields the defective dicubane $[Ni_4(N_3)_4(py_2C(O)(OH))_4]$ (**7**). The reported systems afford an interesting example of multicomponent supramolecular assembly of capsules with nanometric size (~2 nm) and bowls controlled by the alkali cations. The magnetic properties of the rings have been studied, revealing ferromagnetic and antiferromagnetic superechange pathways inside the $\{Ni_6\}$ rings with a $S = 0$ ground state.

Results and Discussion

Structural description.

The supramolecular arrangement of complexes **1**-**5** is based on the common $[Ni_6(CO_3)(N_3)_6(Pz)_3\{py_2C(O)(OH)\}_3]^{2-}$ metallacycle that exhibits the same connectivity and similar bond parameters for the five compounds. Complex **6** shows structural differences that will be described separately. To avoid repetitive text for **1**-**5**, a common description of this fragment will be previously presented. Some of the compounds have two crystallographically independent molecules with very similar bond parameters, so in these cases, the description and bond parameter values correspond to the molecule labelled as A in the crystallographic files.

$[Ni_6(CO_3)(N_3)_6(Pz)_3\{py_2C(O)(OH)\}_3]^{2-}$ metallacycle. One representative labeled plot and the main bond parameters are reported in Figure 1 and Table 1. Complexes **1**-**5** contain a hexagonal arrangement of Ni^{II} cations held together by one μ_6-CO_3^{2-} ligand placed in the center of the $\{Ni_6\}$ planar ring. In addition, the Ni^{II} cations are alternatingly linked by one end-on azido and one pyrazole bridges and one end-on azido and the deprotonated O-donor from one $py_2C(O)(OH)^-$ ligand. The Ni-N-Ni bond angles are slightly larger than 90º and thus, they are lower than the usual angles around 100º typically promoted by end-on azido ligands.[24]

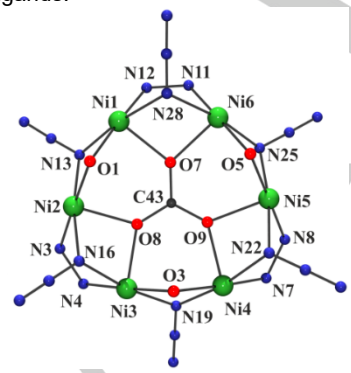

Figure 1. Representative labelled core of the $\{Ni_6\}$ ring for complexes **1**-**5**. Color key for all figures: Ni, green; Li, orange; Na, blue; K, violet; Cs, firebrick; N, navy; O, red; C, gray.

The Ni-O-Ni bond angles are also lower than 96º, being slightly larger those promoted by the O-carbonato donors, Table 1. All the Ni^{II} cations exhibit the same octahedral NiN_4O_2 coordination environment (two N-azide, one N-pz, one N-pyridyl, one O-$py_2C(O)(OH)^-$ and one O-carbonate).

Table 1. Selected bond parameters for one representative $\{Ni_6\}$ ring. The data corresponds to the $[Ni_{12}Na_2]$ complex **2**.

Ni-O (carbonate)		**Ni-O (dpk)**	
Ni(1)-O(7)	2.093(2)	Ni(1)-O(1)	2.086(2)
Ni(2)-O(8)	2.079(2)	Ni(2)-O(1)	2.090(2)
Ni(3)-O(8)	2.059(2)	Ni(3)-O(3)	2.088(2)
Ni(4)-O(9)	2.087(2)	Ni(4)-O(3)	2.042(2)
Ni(5)-O(9)	2.072(2)	Ni(5)-O(5)	2.056(2)
Ni(6)-O(7)	2.078(2)	Ni(6)-O(5)	2.070(2)
Ni-N (azido)			
Ni(1)-N(13)	2.089(2)	Ni(4)-N(22)	2.161(2)
Ni(2)-N(13)	2.094(2)	Ni(5)-N(22)	2.159(3)
Ni(2)-N(16)	2.180(2)	Ni(5)-N(25)	2.096(3)
Ni(3)-N(16)	2.193(2)	Ni(6)-N(25)	2.086(3)
Ni(3)-N(19)	2.113(2)	Ni(6)-N(28)	2.175(3)
Ni(4)-N(19)	2.087(3)	Ni(1)-N(28)	2.139(2)
Ni-N (pyrazole)			
Ni(1)-N(12)	2.037(3)	Ni(4)-N(7)	2.036(3)
Ni(2)-N(3)	2.036(2)	Ni(5)-N(8)	2.029(3)
Ni(3)-N(4)	2.045(3)	Ni(6)-N(11)	2.016(3)
Bond angles			
Ni(1)-N(13)-Ni(2)	91.19(9)	Ni(1)-O(1)-Ni(2)	91.40(2)
Ni(2)-N(16)-Ni(3)	91.17(9)	Ni(3)-O(3)-Ni(4)	94.28(8)
Ni(3)-Ni(19)-Ni(4)	92.3(1)	Ni(5)-O(5)-Ni(6)	92.79(8)
Ni(4)-N(22)-Ni(5)	90.2(1)	Ni(2)-O(8)-Ni(3)	96.89(8)
Ni(5)-N(25)-Ni(6)	91.2(1)	Ni(4)-O(9)-Ni(5)	94.80(7)
Ni(6)-N(28)-Ni(1)	91.7(1)	Ni(6)-O(7)-Ni(1)	95.79(8)

Three $\mu_{1,1}$-N_3 and the three pyrazolate ligands are placed in one side of the main Ni_6 plane whereas the other three $\mu_{1,1}$-N_3 ligands and the three $py_2C(O)(OH)^-$ ligands are placed in the opposite face of this main plane. This arrangement has as a consequence that the six O-donors from the $py_2C(O)(OH)^-$ ligands and the negative charges are placed in the same side of the molecule generating a hydrophilic cavity that can promote H-bonds or to coordinate the alkali cations, as will be described for

each compound. In contrast, the three pyrazolate ligands, coordinated in the opposite side of the ring, generate a cavity with mainly hydrophobic character, Figure 2. This ligands arrangement becomes determinant in the final supramolecular assembly that dictates the nuclearity and shape of the complexes described below.

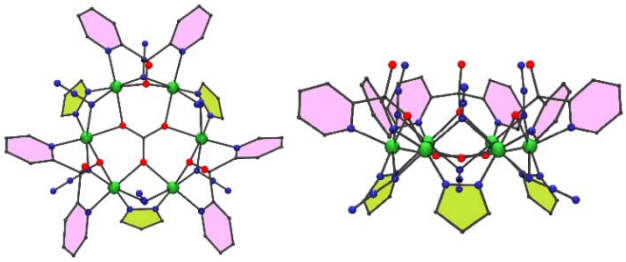

Figure 2. Views of the {Ni_6} ring showing the arrangement of the pyrazole (green) and $py_2C(O)(OH)^-$ ligands (violet) above and below the Ni_6 main plane.

{$(Et_3NH)Li(H_2O)\subset[Ni_6(CO_3)(N_3)_6(Pz)_3(py_2C(O)(OH))_3]\}_2\cdot 0.375H_2O$ (1·0.375 H_2O**).** The centrosymmetric [$Ni_{12}Li_2$] cluster is formed by two hexanuclear {Ni_6} rings, two Li^I, two Et_3NH^+ cations and two water molecules, Figure 3. Each water molecule, placed inside the cavity generated by the two rings, forms two H-bonds with the two deprotonated O3 and O5 donors from the $py_2C(O)(OH)^-$ ligands. The distance between the mean Ni_6 planes is 8.169 Å and the lithium cations are placed quasi equidistant among them (distance main planes to Li^I cations of 4.105 and 4.065 Å). The Li^I cations are placed in a tetrahedral coordination environment linked to the two water molecules and two protonated R-OH groups provided by two $py_2C(O)(OH)^-$ ligands involving the O4 and O6 donors of both rings with very large Li-O distances, larger than 2.7 Å in all cases, Table 2. The water molecules and the donors O2 and O6 from the protonated alkoxo arms contribute to join the two {Ni_6} rings by means of H-bonds (O10···O2', 2.991(9) Å and O2···O6', 3.155(7) Å.

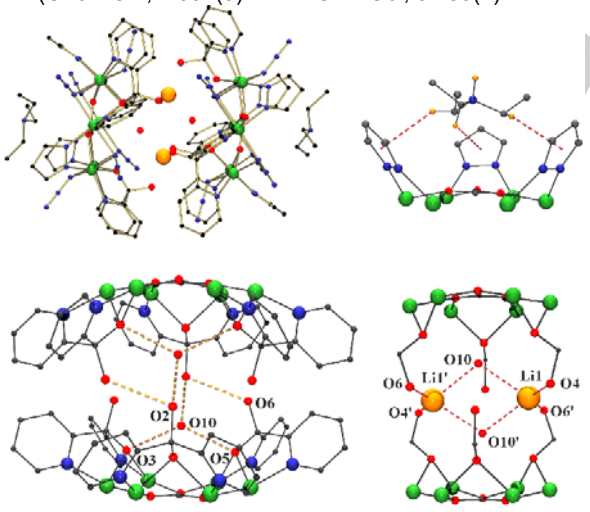

Figure 3. Top, a view of the molecular assembly of compound **1**. The different interactions that contribute to stabilize the system are shown in detail in separate plots: top, CH···π contacts between the Et_3NH^+ cations and the pyrazole rings. Bottom, H-bonds involving the water molecules and the alkoxo arms of the $py_2C(O)(OH)^-$ ligands and the Li^I-O electrostatic interactions.

The external hydrophobic sides of the {Ni^{II}_6} rings interact with the triethylammonium cations by means of weak CH···π contacts with distances ranging between 2.852-3.060 Å among the H-atoms H44D, H46E and H48D and the centroid of the rings.

{$(Et_3NH)Na(H_2O)\subset[Ni_6(CO_3)(N_3)_6(Pz)_3(py_2C(O)(OH))_3]\}_2\cdot CH_3CN\cdot 0.5H_2O$ (2·$CH_3CN\cdot 0.5H_2O$**).** The whole [$Ni_{12}Na_2$] cluster is similar to the lithium one in its general trends, also formed by two hexanuclear {Ni_6} rings, two Na^I and two Et_3NH^+ cations and two water molecules linked by H-bonds to the deprotonated O3 and O5 donors. However, the connectivity inside the capsule is different as a consequence of the larger radius of the alkali cation, Figure 4.

The distance between the mean Ni_6 planes is 8.246 Å and the distance to the Na^I cations to these mean planes is asymmetric (3.212 and 5.034 Å) due to the deeper inclusion of the cations inside the metallamacrocyclic cavity, interacting with one deprotonated O-donor and one μ_3-N-$_{azido}$ atom from the metallacycle. The Na^I cations show an heptacoordinate environment formed by two O-donors of one $py_2C(O)(OH)^-$ (O1 and O2), one $\mu_{1,1,1}$-N_3 ligand (N16) from one of the rings, one alkoxo arm and one $\mu_{1,1,3}$-N_3 ligand from the other ring (O4 and N30), and two water molecules, that act as a bridge between both sodium cations, with a Na-O10-Na' bond angle of 85.83(9)º, Table 2. The additional H-bonds that help to stabilize the structure are limited to the interaction between one –COH arm from one $py_2C(O)(OH)^-$ with one azido ligand from the other ring with O6···N30 distance of 2.684(5) Å.

The external hydrophobic side of the {Ni_6} rings interact with the triethylammonium cations by means of weak CH···π contacts in a similar way than the Li^I complex.

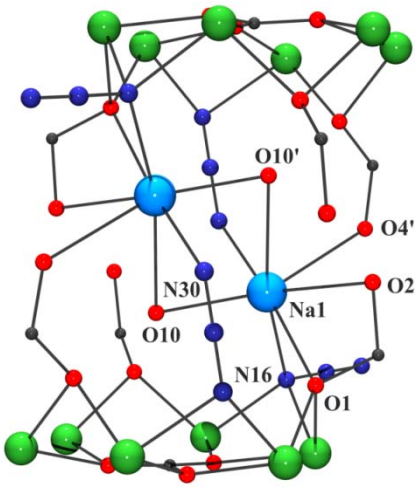

Figure 4. View of the sodium environment and the linkage between rings for complex **2**. The general shape of the molecule and the interactions between the Et_3NH^+ cations and the pyrazole rings are the same than for complex **1**, Figure 3, top.

$(Et_3NH)K(H_2O)_2 \subset [Ni_6(CO_3)(N_3)_6(Pz)_3(py_2C(O)(OH))_3]\cdot 4CH_3CN$ (3·4CH_3CN). The potassium complex contains the same hexanuclear ring than the precedent systems but in this case the complex is a bowl formed by only one ring, one potassium and one triethylammonium cations, Figure 5. The radius of the K^I ion is enough to interact with the inner O-donors of the ring and its position is centered inside the hydrophilic cavity at 2.529 Å over the main {Ni_6} plane. The complicated coordination sphere of the potassium cation contains several sets of donors at different distances: the shorter ones are provided by two water molecules with K-O10 and K-O11 distances of 2.789 and 2.678 Å and the three deprotonated O-donors of the $py_2C(O)(OH)^-$ ligands of the ring, which acts as a tridentate metallacrown with K-O distances in the 2.771-3.061 Å range. Three O-donors from the carbonato ligand are placed at larger distances in the 3.144-3.299 Å range and finally, one N-donor from one $\mu_{1,1,1}$-N_3 azido bridge at 3.286 Å, Table 2. The tridentate interaction of the π-system of the carbonato ligand with one cation is extremely unusual, being reported only in one case for one Cs^I cation with Cs-O distances close to 3.5 Å.[25] The protonated alkoxo arms do not interact with the potassium cation and they are involved in intramolecular H-bonds with one of the coordinated water molecules (O10-O2 2.807 Å) or with the azido ligands (O6-N30 3.108 Å and O4-N18 2.952 Å).

The Et_3NH^+ countercation is placed on the opposite hydrophobic side of the {Ni_6} cycle and interacts with the pyrazole rings by means of CH···π contacts in a similar manner to the above described complexes.

$(Et_3NH)\{Cs(H_2O) \subset [Ni_6(CO_3)(N_3)_6(Pz)_3(py_2C(O)(OH))_3]\cdot 2CH_3CN\cdot H_2O$ (4·2$CH_3CN\cdot H_2O$).

The cesium complex is closely related to the potassium case but due to the larger radius of the cation it reaches to interact with all the donors of the cavity, including the protonated alkoxo arms from the $py_2C(O)(OH)^-$ ligands, Figure 6. The distance from the Cs^I cation to the main {Ni_6} plane is 2.840 Å. The coordination environment of the cation consist of the three deprotonated O-donors of the metallacrown (Cs-O in the 3.032-3.126 Å range), the three protonated –COH arms (Cs-O in the 3.460-3.581 Å range), the π system of the carbonate (Cs-O in the 3.467-3.528 Å range), three N-atoms from the three azido ligands (Cs-N in the 3.418-3.612 Å range) and one water molecule (Cs-O10 3.148 Å) resulting an unusual $CsO_{10}N_3$ environment, Table 2.

The interaction of the Et_3NH^+ countercation with the hydrophobic *exo* cavity of the ring is similar to the precedent cases **1**-**3**.

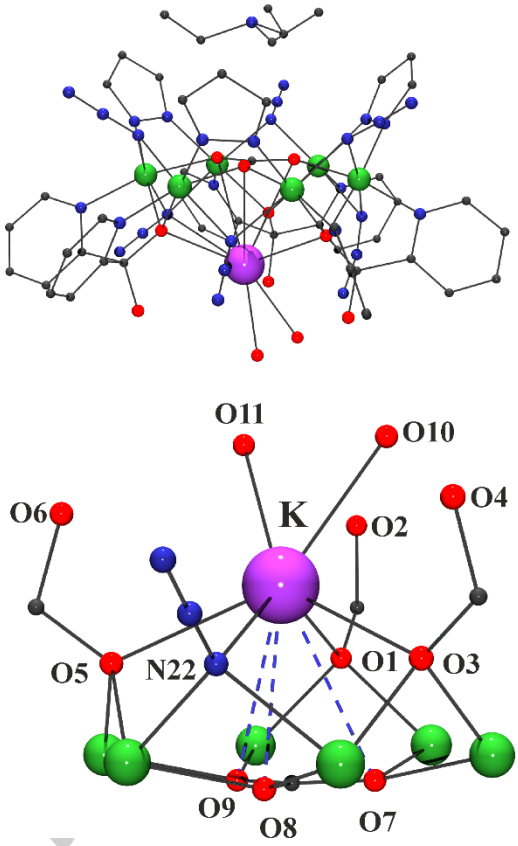

Figure 5. Top, a view of the molecular assembly of compound **3**. Bottom, coordination environment for the potassium cation. The interactions between the Et_3NH^+ cations and the pyrazole rings are the same than the previous complexes **1** – **2**.

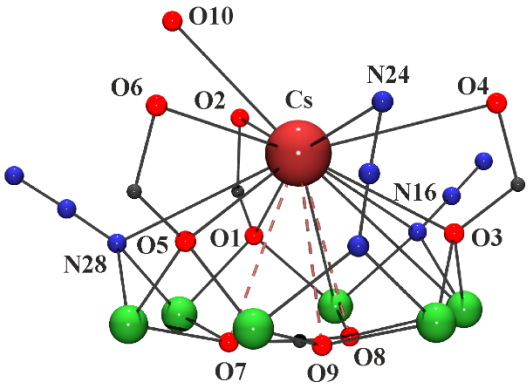

Figure 6. Coordination environment for the cesium cation for compound **4**. The interactions between the Et_3NH^+ cations and the pyrazole rings are the same than the previous complexes **1** – **3**.

Table 2 Bond distances (Å) for the alkali coordination environment in complexes **1**-**4**.

Complex (1)			
Li-O10	2.71(1)	Li-O4	2.73(1)
Li-O10'	2.78(2)	Li-O6	2.73(1)
Complex (2)			
Na-O10	2.323(3)	Na-O10'	2.585(3)
Na-O1	2.454(2)	Na-O2	2.542(3)
NaO4'	2.748(3)	Na-N16	2.576(3)
Na-N30'	2.460(4)		
Complex (3)			
K-O10	2.789(14)	K-O11	2.677(13)
K-O1	3.061(4)	K-O7	3.299(4)
K-O3	2.874(4)	K-O8	3.144(4)
K-O5	2.771(4)	K-O9	3.260(3)
K-N22	3.178(5)		
Complex (4)			
Cs-O1	3.031(3)	Cs-O2	3.460(4)
Cs-O3	3.085(3)	Cs-O4	3.570(4)
Cs-O5	3.126(5)	Cs-O6	3.581(5)
Cs-O7	3.521(3)	Cs-N16	3.425(4)
Cs-O8	3.467(3)	Cs-N24	3.456(9)
Cs-O9	3.527(3)	Cs-N28	3.632(5)
Cs-O10	3.149(5)		

{(Et$_3$NH){M(H$_2$O) ⊂ [Ni$_6$(CO$_3$)(N$_3$)$_6$(Pz)$_3$(py$_2$C(O)(OH))$_3$]}$_2$ M = Na, K (5). The structure consists of co-crystallized [Ni$_{12}$Na$_2$] and [Ni$_{12}$K$_2$] capsules in 1:1 ratio, Figure 7. The structure of the two capsules is closely related to the [Ni$_{12}$Na$_2$] complex **2** and thus, their descriptions are referred to the above provided details.

The sodium capsule is similar to complex **2** but in this case excluding the interaction with the azido ligand from the neighboring ring and thus, the coordination around the sodium cation is reduced to an hexacoordinated environment. With the exception of the larger Na-O1 distance, the Na-O or Na-N bond distances are slightly shorter than for **2**. The potassium capsule shows an heptacoordinated environment, fully analogous to complex **2**, with the K-O and K-N bond distances logically larger than the sodium case, Table 3. Comparison with the potassium bowl **3** shows a lower coordination number associated to shorter K-O and K-N bond distances and the loss of the K-O contacts with the carbonate anion.

The M-O10-M bond angles take the values of 105.50(5)º for the sodium and 86.25(5)º potassium capsules and the {Ni$_6$} interplane distance is similar in both cases, 8.169 Å (Na^I capsule) or 8.155 Å (K^I capsule). The H-bonds between the water molecules and the deprotonated O-donors from the py$_2$C(O)(OH)$^-$ ligands and the contacts between the rings are also like in the case of complex **2**. As in the previous cases, the Et$_3$NH$^+$ countercations are placed on the opposite hydrophobic side of the {Ni$_6$} cycles interacting with the pyrazole rings by means of CH···π contacts.

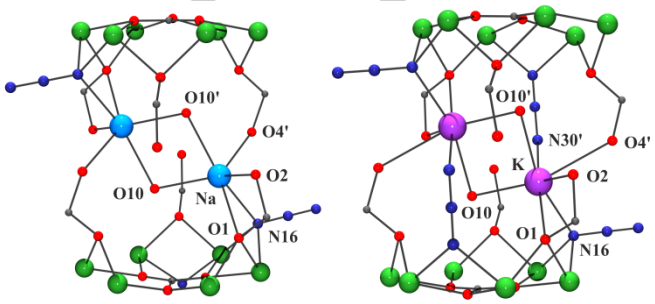

Figure 7. A view of the core and the coordination environment for the sodium (left) and potassium (right) cations for compound **5**. The interactions between the Et$_3$NH$^+$ cations and the pyrazole rings are the same than the previous complexes **1** – **4**.

Table 3 Bond distances (Å) for the alkali coordination environment for the sodium and potassium complexes **5**.

Complex (5) Na^I capsule			
Na-O10	2.297(1)	Na-O10'	2.457(1)
Na-O1	2.634(1)	Na-O2	2.402(1)
NaO4'	2.637(1)	Na-N16	2.565(1)
Complex (5) K^I capsule			
K-O10	2.343(1)	K-O1O'	2.522(2)
K-O1	2.408(1)	K-O2	2.557(1)
K-O4'	2.755(1)	K-N16	2.568(2)
K-N30'	2.430(2)		

(Me$_4$N){K(H$_2$O) ⊂ [Ni$_6$(CO$_3$)(N$_3$)$_6$(Pz)$_3$(py$_2$C(O)(OH))$_3$] ·2.5CH$_3$CN (6·2.5CH$_3$CN**).** The structure of complex **6** is similar in general trends to the above described systems but the change of the base (Me$_4$NOH instead Et$_3$N) induces specific changes in the core. The main difference lies in the arrangement of the ligands with respect to the {Ni$_6$} rings: one of the azido and one of the py$_2$C(O)(OH)$^-$ ligands changed its orientation and consequently there are four azido ligands and two py$_2$C(O)(OH)$^-$ ligands placed on the hydrophilic side of the {Ni$_6$} ring and, two azido, the three pyrazoles and one py$_2$C(O)(OH)$^-$ ligands on the hydrophobic *exo* cavity, Figure 8, top and Table 4. The

potassium cation is not placed over the centroid of the ring due to this asymmetry and is coordinated to only two deprotonated O-donors and the two alkoxo arms of the $py_2C(O)(OH)^-$ ligands, one $\mu_{1,1,1}$-N_3, two $\mu_{1,1,3}$-N_3 bridges, one of the O-donors from the carbonate anion and finally to one of the alkoxo arms from the neighbor molecule, Figure 8, middle. The tetramethylamonium cation is placed inside the cavity formed by the pyrazole rings in a similar manner than in previous cases Figure 8, middle. The reversed $py_2C(O)(OH)^-$ ligand has the protonated alkoxo arm directed to the external side of the molecule and it is linked to the potassium cation of the neighbor molecule, generating an one dimensional arrangement of clusters in the network, Figure 8, down.

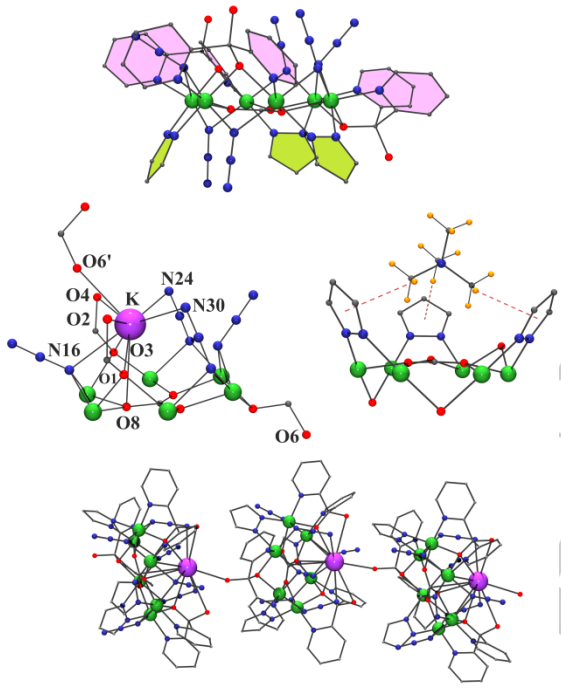

Figure 8. Top, view of the $\{Ni_6\}$ metallacycle showing the pyrazole (green) and pyridyl rings of the $py_2C(O)(OH)^-$ ligands (violet) and the arrangement of the azido and $py_2C(O)(OH)^-$ ligands respect the Ni_6 main plane for complex **6**. Middle left, a view of the coordination environment for the potassium cation and the CH···π interaction of the Me_4N^+ cations (right). Bottom, 1D arrangement of clusters linked by one of the diol arms.

Table 4 Selected bond distances (Å) and bond angles (deg.) for the $\{Ni_6\}$ ring and the coordination environment of the potassium cation for complex **6**.

Ni1-O1-Ni2	93.7(1)	Ni1-N13-Ni2	91.8(2)
Ni3-O3-Ni4	94.7(1)	Ni2-N16-Ni3	91.7(1)
Ni5-O5-Ni6	92.3(1)	Ni3-N19-Ni4	92.4(1)
Ni1-O7-Ni6	94.1(1)	Ni4-N22-N5	90.3(1)
Ni2-O8-Ni3	95.9(1)	Ni5-N25-Ni6	88.1(1)
Ni4-O9-Ni5	96.8(1)	Ni1-N28-Ni6	90.4(1)
K-O1	2.805(3)	K-N16	2.865(4)
K-O3	2.875(3)	K-N24	3.112(5)
K-O2	3.289(4)	K-N30	3.075(5)
K-O4	3.346(3)	K-O8	3.189(3)
K-O6'	2.948(3)		

$[Ni_4(N_3)_4(py_2C(O)(OH))_4]\cdot 3CH_3CN$ (7·$3CH_3CN$). The centrosymmetric complex **7** consists of four Ni^{II} cations held together by four $py_2C(O)(OH)^-$ ligands and two azido bridges, Figure 9. The coordination sphere of Ni(1) and symmetry related cation is fulfilled with one terminal azido ligand. Two of the $py_2C(O)(OH)^-$ ligands provide a μ-O bridge between Ni(1) and Ni(2) whereas the other two link Ni(1), Ni(2) and Ni(2') by means a μ_3-O bridge. The protonated arms of the $py_2C(O)(OH)^-$ ligands promote strong H-bonds with the terminal azide (O2···N7, 2.802(4) Å) and the μ_3-O donor (O4···O3 2.644(2) Å).

Tetranuclear Ni^{II} clusters derived from dipyridylketone are well known and complex **7** shows the same core and connectivity than similar reported complexes[12-16] and thus, no further description is needed. The crystallographic parameters and bond parameters are supplied in ESI, Tables S2 and S3.

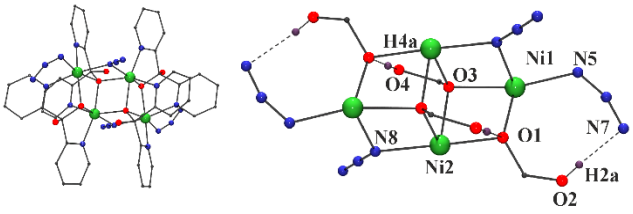

Figure 9. Left, a view of the molecular unit of complex **7**. Right, labelled core. H-bonds are plotted as dotted bonds.

Synthetic aspects

The synthesis of the reported systems requires a careful design to generate the conditions that allow to the stabilization of the capsules or bowls by means of a wide variety of supramolecular interactions. The main factors to take into account involve the carbonate anion, the pyrazolate coligand, the azido source and the base employed to deprotonate the ligands. As result, the self assembly of up to 44 individual fragments yields the nanometric capsules, Figure 10.

i) ***The carbonate anion***. The carbonato ligand is a very good donor that can bind metallic cations in a wide variety of coordination modes that comprises denticities from the monodentate up to the μ_{10}-CO_3^{2-} modes. The μ_6-CO_3^{2-} bridging mode becomes interesting because can generate planar hexanuclear systems in which acts as a templating anion with a variety of cations (up to 42 entries in the CCDC database). Among them, the Ni^{II} cation is prone to generate isolated or decorated metallamacrocycles[26-30] in which the resulting ring is templated by the carbonate anion, usually obtained by reaction of the basic mixture of the reagents with atmospheric CO_2. Following this procedure, the CO_2 capture for compounds **1**-**6** was favored by vigorous stirring of the basic reaction solutions at open air during some hours followed by the slow evaporation also at open air.

ii) ***Pyrazolate coligand***. The employment of the monoanionic pyrazolate coligand is crucial to reach the anionic $\{Ni_6\}$ rings with different *endo* and *exo* binding sites. In the reported **1**-**5** systems all the O-donors from the $py_2C(O)(OH)^-$ ligands are placed in the same side of the ring whereas the pyrazolate ligands are placed on the opposite side, generating one metallamacrocycle with one hydrophilic and one hydrophobic cavities that are able to coordinate cations with so different character such spherical alkali cations or alkylamines. The different coordination observed for complex **6** shows the change of position between one azido and one $py_2C(O)(OH)^-$ ligand, resulting a less symmetric ring but keeping the same character for the *endo* and *exo* binding sites.

iii) ***Cation size and charge***. The size of the cation along the alkali group is the most evident factor that determines the nuclearity of the complexes **1**-**6**. The larger ones, which can interact with the charged O-donors of the metallacycle, tend to the bowl shape whereas the smaller ones, that can not directly interact with the metallacycle, tend to form capsules. The border between both kind of structures was experimentally found in the Na^I/K^I limit and thus, we tried the reaction in the presence of both cations in 1:1 ratio with the aim to determine the preferred structure: the resulting complex **5** shows the co-crystallization of sodium and potassium capsules closely related to the sodium capsule **2**. This result confirms that the limit of cation size between both structures corresponds to the potassium cation that is able to produce bowls like **3** or **6** or a capsule like compound **5**, in which the system, probably by packing optimization, is adapted to the sodium structure. In light of the cavity size, we performed trial reactions in the presence of cations with ionic radius similar to the sodium or potassium ions in some cases. All reactions with the monovalent Ag^I or the divalent Mg^{II} or Ca^{II} cations were performed in absence of alkali cations and were unsuccessful in all cases, resulting poorly crystalline compounds that do not show the characteristic IR spectra of the $\{Ni_6\}$ ring, pointing out the selectivity of the systems towards the alkali cations.

iv) ***Azido ligand***. Sodium azide is the main reagent in cluster azido chemistry in spite it is only soluble in water or slightly soluble in methanol. Its poor solubility in the most of the common solvents other than water or methanol, becomes a synthetic problem that usually requires the addition of solid NaN_3 in large excess in order to dissolve the azido anion by coordination to the soluble cations. To generate series of complexes with cations with different size it was necessary to generate mixtures in which the adequate Li^I, Na^I, K^I or Cs^I ions could be added avoiding competence between them. For the Na^I and K^I cases this target is easy to reach employing as starting reagent the corresponding azide salt (NaN_3 or KN_3). In contrast, for reactions in which the only presence of Li^I, Cs^I, Mg^{II} or Ca^{II} ions was desired, it was necessary to employ a different and unusual strategy such the addition of the tetrabuthylammonium azide salt as azido source and the addition of the corresponding alkali or alkaline perchlorates. The employment of $(Bu_4N)N_3$ in cluster chemistry is advantageous from two points of view: it is soluble in all common solvents including those that are poorly polar and spread the possibilities of cluster azido chemistry to reaction mediums that are usually unreachable.

,

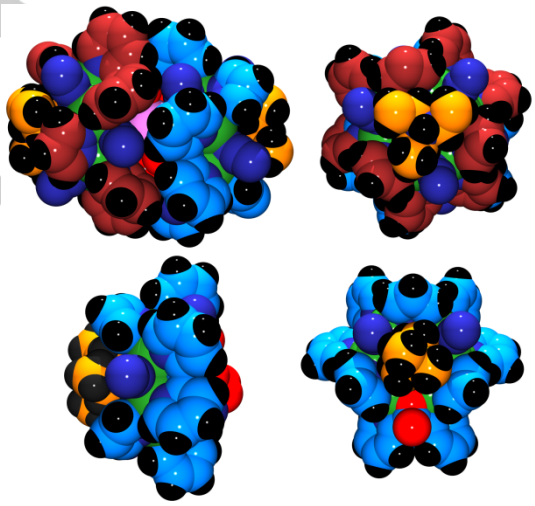

Figure 10. Top, lateral and axial views of the capsules formed for compounds **1**, **2** and **5**. Bottom, lateral view of the bowls formed for compounds **3** and **4** and the axial view for the bowl **6** showing the coordination of the alkylated co-cation and the reversed $py_2C(O)(OH)^-$ ligand. Color key: C-atoms belonging to the metallamacrocycles, firebrick and light blue; C-atoms belonging to the alkylated co-cations, orange; H-atoms, black.

v) ***Co-cations***. The base employed to deprotonate the HPz and $py_2C(OH)_2$ ligands shows to be relevant to stabilize the capsules or bowls. In complexes **1**-**5** the Et_3NH^+ cation is coordinated on the hydrophobic face of the metallacycles and the change of the of Et_3N by the $Me_4N(OH)$ base shows to be not relevant for the stability of the system because in complex **6** the Me_4N^+ cation

becomes coordinated in the same hydrophobic cavity forming similar CH···π interactions. However, even maintaining the bowl formation, the change of the co-cation is not innocent and promotes a different arrangement of the ligands, reversing the position of one of the azido and one of the $py_2C(O)(OH)^-$ ligands as has been above described.

Performing the same reaction that allows to complex **2** but employing NaOMe as base, Na^I were the only cations present in the reaction medium and the lack of the alkylated co-cations changes completely the resulting molecule, that consist of one conventional {Ni_4} cluster with butterfly topology (compound **7**), pointing out the crucial role of the employment of alkylammonium counteractions to stabilize the complexes by linkage to the *exo* hydrophobic face of the rings. It is remarkable that the carboxylato related system reported by Tong. et al.[22] was stable exclusively for the potassium cation.

Supramolecular interactions

The self assembled complexes **1**-**6** are built by a wide variety of supramolecular interactions that contribute to the stability of the systems.

As was above described the carbonate anion determines the topology of the nickel rings which are templated by the μ_6-CO_3^{2-} coordination mode of the anion that places the Ni^{II} cations at the adequate distance (~3 A) to link the pyrazolate, end-on azido or alkoxo bridging ligands. The resulting metallamacrocycle acts as a ligand, coordinating the alkali cations by means of the pendant protonated alkoxo arms and/or by means of the deprotonated μ-O donors in which case, the ring acts as a true metallacrown[31] linking the larger cations (K^I and Cs^I, compounds **3**, **4** and **6**).

The H-bonds play a crucial role in the stability of the capsules **1**, **2** and **5** helping to join the two moieties of the molecules. The complementary H-bonds are promoted by the bridging water molecules which are anchored to the O-donors of the ring and the protonated alkoxo arms that in addition, promotes inter-ring interactions, Figure 3, bottom.

CH-π interactions are weaker than π-π stacking or H-bonds but this kind of contacts are favored by the presence of electronegative atoms in aromatic heteroatom rings and the intermolecular contacts usually contribute to supramolecular arrangements in the network. Pyrazole rings have a wide supramolecular chemistry focused in its ability to participate in H-bonds[32] but also are very prone to establish CH-π interactions (around one third of the pyrazole systems reported in CCDC database). In this case, compounds **1** – **6** have three pyrazole rings placed at ~120º and they become complementary with the alkyl arms from the $HNEt_3^+$ or the NMe_4^+ cations, also placed at 120º between them. These cations are coordinated to the hydrophobic side of the rings by means of three weak CH-π contacts, more symmetric for **1** – **5**(Na), with distances from the H-atom to the centroid of the pyrazole rings around 2.9 Å and asymmetric for compounds **5**(K) and **6**, with two shorter H-centroid distances of 2.615 and 2.752 Å and one larger distance of 3.104 Å, ESI Table S1. Noteworthy, despite the large number of CH-π contacts that can be found in the literature that involve alkyl, phenyl or solvents such CH_2Cl_2, only one recent example has been reported for the triangular interaction with NR_3 molecules and three pyrazole rings.[33]

Finally, the alkali cations play an important role and promote different kind of interactions in function of its ionic radius. On one side, the cations with larger coordination spheres such K^I and Cs^I prefer the bowl topology found in **3**, **4** and **6** because they can interact more easily with the negatively charged donors such the μ_3-N_3 or the deprotonated O-atoms from the $py_2C(O)(OH)^-$ ligands and even, are able to stablish a contact with the π system of the carbonate anion. On the other side, sodium cation, with a more limited coordination sphere, interact with donors from two rings determining the stronger linkage between them and resulting the capsule topology.

The Li^I cations in complex **1** exhibit a tetracoordinated environment with four very large Li···O distances that lies in the short 2.713-2.835 Å range. The most usual Li-O distances for tetracoordinated lithium cations are comprised in the 1.9-2.0 Å range (CCDC database, ~1500 entries) and the Li-O distances up to 2.70 Å are exclusively found for large coordination numbers with poor donors, as can be those found for octacoordinated crown ether complexes like $[Li(12Cr4)2]^+$. The Li-O distances found in complex **1** are the largest reported to date for tetracoordinated lithium cations and thus, the supramolecular interaction that helps to join both rings should be assumed as a ionic interaction and the cations should be assumed as trapped inside a negatively charged electrostatic cavity.

Magnetic properties

The magnetic properties for complexes **1**-**4** and **6** were measured in powdered samples in the 2-300 K range of temperature. The $\chi_M T$ product *vs.* temperature plots for complexes **1**-**4** are shown in Figure 11. As can be expected from the similar bond parameters found in their structures, all complexes show a similar magnetic response that is related with the interactions inside the magnetically isolated Ni_6 rings. The room temperature values for {Ni_6} unit range between 6.89-7.43 $cm^3 \cdot mol^{-1} \cdot K$, in agreement with the expected value for six isolated S = 1 local spins (6.00 $cm^3 \cdot mol^{-1} \cdot K$) increased due to g values up to the usual 2.15-2-25 range. The $\chi_M T$ values slightly increases on cooling up to maximum values in the 45 – 70 K range and below these maxima decrease tending to zero at low temperatures. The shape of the plots evidences dominant ferromagnetic interactions at higher temperatures and overall antiferromagnetic response at low temperature. The presence of maxima of susceptibility around 10 K imply an S = 0 ground state in all cases. In good agreement, magnetization measurements show a continuous increment up to low values, far from saturation, in the range of 3.0-5.0 MN_β, that corresponds to the progressive population of low-lying spin states close to the S = 0 ground state, see ESI Figure S1.

From the structural information, the six Ni^{II} cations are related by four different superexchange pathways into the hexanuclear rings, two of them mediated by triple $\mu_{1,1}$-N_3/μ-O/*syn-syn*-CO_3^{2-} or $\mu_{1,1}$-N_3/μ-O/ μ-Pz^- bridges and the other two, mediated exclusively by the carbonato ligand with *syn-anti*-CO_3^{2-} or *anti-*

anti-CO_3^{2-} bridges. The complete coupling scheme derived from these interactions is shown in Scheme 2 and the derived Hamiltonian is:

$$H = -2J_1(S_1 \cdot S_2 + S_3 \cdot S_4 + S_5 \cdot S_6) - 2J_2(S_2 \cdot S_3 + S_4 \cdot S_5 + S_1 \cdot S_6) - 2J_3(S_1 \cdot S_3 + S_1 \cdot S_5 + S_2 \cdot S_4 + S_2 \cdot S_6 + S_3 \cdot S_5 + S_4 \cdot S_6) - 2J_4(S_1 \cdot S_4 + S_2 \cdot S_5 + S_3 \cdot S_6)$$

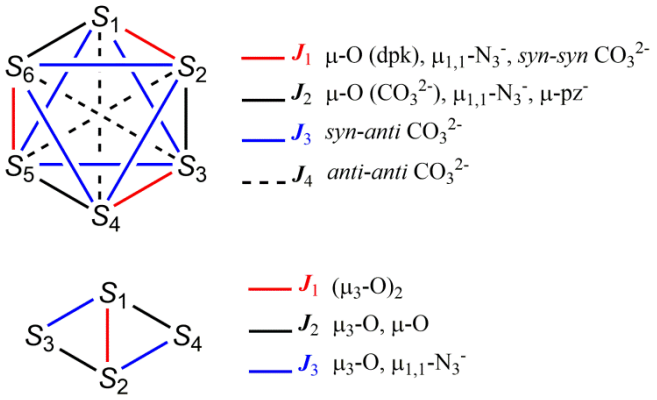

Scheme 2. Top, coupling scheme for complexes **1**-**4** and **6**. Bottom, coupling scheme for complex **7**.

Excellent fits of the experimental data for complexes **1**-**4** and **6** were obtained from the application of this four-*J* Hamiltonian. The best fit parameters are summarized in Table 5.

Table 5. Best fit parameters for the magnetic measurements of complexes **1**-**4** and **6**.

Complex	J_1	J_2	J_3	J_4	*g*	$R(\chi_M T)$
(**1**)	11.0	-6.9	2.6	-0.7	2.15	$1.5 \cdot 10^{-5}$
(**2**)	8.8	-6.1	2.1	-0.9	2.16	$1.8 \cdot 10^{-5}$
(**3**)	12.8	-8.4	4.6	-0.4	2.13	$7.4 \cdot 10^{-5}$
(**4**)	9.8	-7.5	4.1	-0.2	2.10	$2.5 \cdot 10^{-5}$
(**6**)	7.0	-6.2	2.3	-0.8	2.04	$5.1 \cdot 10^{-6}$

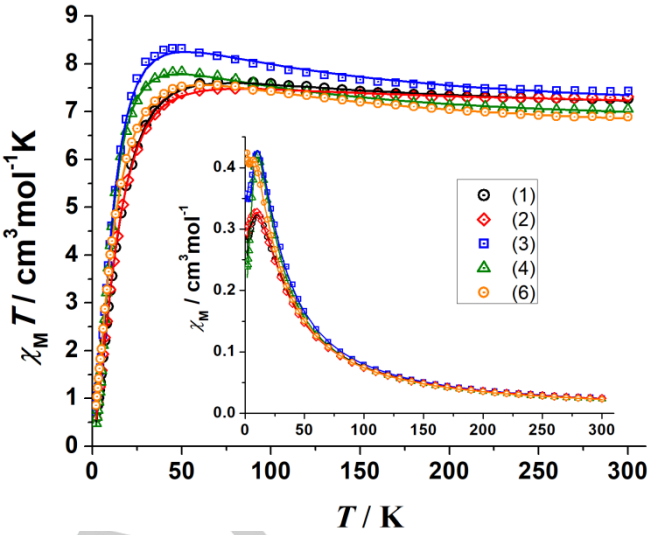

Figure 11. $\chi_M T$ *vs.* *T* plot for complexes **1**-**4** and **6**. Inset, χ_M *vs.* T plots showing the maxima of susceptibility.

The *J* values agree with the expected sign and absolute value for the corresponding superexchange pathways. The related metallacycle reported by Tong et al.[22] contains peripheral $\mu_{1,1}$-N_3/μ-O/*syn*-*syn*-CO_3^{2-} and $\mu_{1,1}$-N_3/μ-O/*syn*-*syn*-$MeCO_2^-$ bridges and exhibits a full ferromagnetic response. The bond parameters for the N_3/μ-O/*syn*-*syn*-CO_3^{2-} pathway are very close to those found in **1**- **6** and by comparison, ferromagnetic coupling, parametrized as J_1, should be assigned univocally to this pathway. DFT calculations shown that the predicted interaction mediated by end-on azido bridges in Ni(II) complexes is ferromagnetic, with a maximum positive value around a Ni-N-Ni bond angle of 104°.[11,34] 1,2-diazines promote antiferromagnetic interactions[35-37] and they are countercomplementary[38] with the azido or oxo bridges reducing the ferromagnetic interactions. and thus, the combination of the weaker ferromagnetic component promoted by the azido bridge with a Ni-N-Ni bond angle around ~91° (Table 1), with the countercomplementary pirazolate bridge agree with the antiferromagnetic character of the $\mu_{1,1}$-N_3/μ-O/*syn*-*syn*-Pz^- pathway parametrized as J_2. This observation shows the very fine details that determine the magnetic properties in polynuclear clusters, since the seemingly minor change from pyrazolate ligands to acetato ligands (from reference 22) in the same metal core leads to a complete reversal of the magnetic ground state from an $S = 0$ due to competing ferromagnetic/antiferromagnetic interactions, to an $S = 6$ due to dominant ferromagnetic interactions.

It is well established that the *syn*-*anti*-CO_3^{2-} pathway promotes weak ferromagnetic coupling and that the *anti*-*anti*-CO_3^{2-} promotes quasi negligible interactions[39-42] as was found for J_3 and J_4. Fits discarding J_4 gave practically the same values for the remainder constants but trials to fit the experimental data discarding J_3 gave worse reproduction of the experimental data, indicating that should be taken into account in the fit procedure.

The $\chi_M T$ product *vs.* temperature for complex **7** shows a room temperature value of 5.92 $cm^3mol^{-1}K$, larger than the spin only

value of 4.00 $cm^3mol^{-1}K$ expected for four S = 1 non interacting spins (g = 2.00), Figure 12. On cooling, the $\chi_M T$ value increase continuously up to a maximum value of 11.9 $cm^3mol^{-1}K$ at 15 K. Below this temperature, the plot decay down to a value of 8.96 $cm^3mol^{-1}K$ at 2 K, suggesting a dominant ferromagnetic interaction with a S = 4 ground state. Fit of the experimental data was performed on the coupling scheme shown in Scheme 2, employing the Hamiltonian:

$$H = -2J_1(S_1 \cdot S_2) - 2J_2(S_1 \cdot S_4 + S_2 \cdot S_3) - 2J_3(S_1 \cdot S_3 + S_2 \cdot S_4)$$

and including a D_{ion} term to fit the low temperature decay. The best fit parameters were J_1 = +7.3 cm^{-1}, J_2 = +17.7 cm^{-1}, J_3 = +13.3 cm^{-1}, D_{ion} = 6.4 cm^{-1} and g = 2.24. The S = 4 ground state was confirmed by the fit of the reduced magnetization plot that gave a $D_{S=4}$ = -0.39 cm^{-1} and g = 2.23. Alternate current measurements do not show out-of-phase signals. The topology and magnetic response fully agree with the well-studied similar complexes derived from Ni^{II}/dpk/N_3^- reported in the literature[12-16].

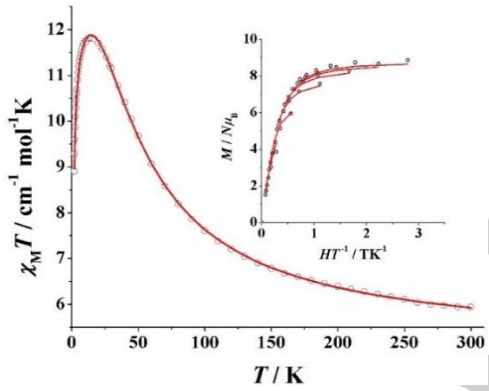

Figure 12. $\chi_M T$ *vs.* T plot for complexes **7**. Inset, reduced magnetization plot showing the non-superimposable magnetization as consequence of the zero-field-splitting of the S = 4 ground state.

Conclusions

As a conclusion, we reported a synthetic strategy for host-guest supramolecular structures bases on hexanuclear Ni^{II} metallacrowns that yielded series of nanometric capsules and bowls controlled, as main factor, by the size of the alkali cations. The reported complexes are an example of supramolecular self-assembled systems by the synergic effect of a variety of intermolecular interactions (template, H-bonds, CH-π, weak coordination bonds, electrostatic), that allows the stabilization of nanocapsules of bowls with multiple *endo*- and *exo*-guests. The *endo*-lithium cations provide a unique example of two lithium cations inside an electrostatic box. The alkyl counteraction has a determinant paper on the stabilization of the assemblies and its role will be explored in the characterization of future systems. Magnetic measurements confirm ferromagnetic and antiferromagnetic pathways inside the $\{Ni_6\}$ ring, with a S = 0 ground state.

Experimental Section

Experimental Details.

IR spectra (4000-400 cm-1) were recorded using a Bruker IFS-125 FT-IR spectrometer with samples prepared as KBr pellets. Variable-temperature magnetic studies were performed using a MPMS-5 Quantum Design magnetometer operating at 0.03 T in the 300-2.0 K range. Diamagnetic corrections were applied to the observed paramagnetic susceptibility using Pascal's constants. Analysis of the magnetic data were performed with PHI program.[43] Quality of the fits were parametrized as the $R = (\chi_M T_{exp} - \chi_M T_{calc})^2/(\chi_M T_{exp})^2$ factor. The yield of the syntheses was for all compounds around a 40-75% of crystalline product that was employed for the instrumental measurements and air dried for the elemental analysis.

Single-crystal X-ray crystallography

Prism-like specimens of **1** - **7** were used for the X-ray crystallographic analysis. The X-ray intensity data were measured on a D8-Venture system equipped with a multilayer monochromator and a Mo microfocus (λ = 0.71073 Å). The frames were integrated with the Bruker SAINT software package using a narrow-frame algorithm. The final cell constants were based upon the refinement of the XYZ-centroids of reflections above 20 σ(I). Data were corrected for absorption effects using the multi-scan method (SADABS). The structures were solved using the Bruker SHELXTL Software Package, and refined using SHELXL.[44] Details of crystal data, collection and refinement are summarized in Table 6 for **1**-**6** and ESI Table S2 for **7**. Analysis of the structures and plots for publication were performed with Ortep3[45] and POVRAY programs.

CCDC 1942681 (**1**), 1996428 (**2**), 1996425 (**3**), 1996426 (**4**), 1996427 (**5**), 1996430 (**6**) and 1996429 (**7**) contain the supplementary crystallographic data for this paper. Thee data are provided free of charge by the Cambridge Crystallographic Data centre.

Warning: azide and perchlorate salts are potentially explosive; such compounds should be synthesized and used in small quantities, and always treated with the maximum care. All IR spectra for **1**-**6** are practically identical and in ESI Figure S2 some representative spectra are shown.

Table 6. Crystal data and structure refinement details for the *X*-ray structure determination of compounds **1**–**6**.

	1	2	3	4	5	6
Formula	$C_{49}H_{54.75}LiN_{31}Ni_6O_{10.38}$	$C_{49.5}H_{53.5}N_{31.25}NaNi_6O_{10.375}$	$C_{57}H_{68}KN_{35}Ni_6O_{11}$	$C_{53}H_{56}CsN_{33}Ni_6O_{11}$	$C_{49}H_{52}K_{0.5}N_{31}Na_{0.5}Ni_6O_{10}$	$C_{57.5}H_{60.75}KN_{36.25}Ni_6O_9$
FW	1603.18	1627.48	1810.82	1816.47	1618.42	1795.03
System	Triclinic	Triclinic	Monoclinic	Monoclinic	Triclinic	Orthorhombic
Space group	P -1	P -1	P21	P21	P -1	Pbcn
a/Å	16.9870(9)	17.268(2)	11.1161(4)	11.1572(4)	16.878(2)	32.648(1)
b/Å	18.1041(9)	18.185(2)	18.8452(8)	18.9272(7)	17.634(2)	19.6664(6)
c/Å	23.780(1)	23.758(3)	19.1705(8)	19.0449(7)	23.752(2)	25.623(1)
α/deg.	95.640(2)	94.354(5)	90	90	95.967(4)	90
ß/deg.	99.050(2)	99.494(5)	100.981(1)	99.866(1)	98.460(4)	90
γ/deg.	99.754(2)	99.250(5)	90	90	99.043(4)	90
V/ Å3	7058.8(6)	7222(2)	3942.4(3)	3962.3(3)	6847(1)	16452(1)
Z	4	4	2	2	4	8
T, K	303(2)	254(2)	100(2)	100(2)	100(2)	100(2)
λ(MoKα), Å	0.71073	0.71073	0.71073	0.71073	0.71073	0.71073
ρ_{calc}, g·cm^{-3}	1.509	1.497	1.525	1.523	1.570	1.449
μ(MoKα), mm^{-1}	1.641	1.611	1.536	1.921	1.725	1.467
Flack param.	----	----	0.000(2)	0.03(1)	----	----
R	0.0577	0.0471	0.0320	0.0388	0.0267	0.0499
ωR^2	0.1542	0.1286	0.0893	0.1048	0.0727	0.1389

The reported compounds were synthesized from a common mixture prepared as follows: To a violet solution of $Ni(ClO_4)_2{\cdot}6H_2O$ (0.36 g, 1.00 mmol) dissolved in 20 mL of acetonitrile were added solid dipyridylketone (0.092g, 0.5 mmol) and solid pyrazole (0.052 g, 0.75 mmol).

Compounds **2** and **3**: to the common solution it was added triethylamine (0.150g, 1.5 mmol) and sodium azide (0.065 g, 1.0 mmol) (compound **2**) or potassium azide (0.81 g, 1mmol) (compound **3**) and the resulting mixture was maintained with continuous stirring at open air during three hours. Slow evaporation of the resulting blue solutions produces well-formed crystals in 2-3 days in 75% yield. Anal. calculated/found (%) for **2**: C, 36.49/36.6; H 3.43/3.5; N 26.86/26.7 and **3**: C, 37.81/37.0; H 3.79/3.8; N 27.08/26.7.

Compounds **1** and **4**: to the common solution it was added triethylamine (0.150g, 1.5 mmol), tetrabutylamonium azide (0.28 g, 1.0 mmol) and lithium perchlorate (0.058 g, 0.5 mmol, compound **1**) or caesium perchlorate (0.116 g, 0.5 mmol, compound **4**) and maintained with continuous stirring at open air during three hours. The resulting solutions were allowed to stand in a closed vial for 1-2 days and a reddish precipitate was removed by filtration. Slow evaporation of this solution gives well-formed crystals after some days in 50% yield. Anal. calculated/found (%) for **1**: C, 36.71/37.2; H 3.44/3.3; N 27.09/26.8 and **4**: C, 34.93/34.4; H 3.43/3.6; N 25.36/24.9.

Compound **5**: was prepared following the same procedure than for **2** – **3** but with a 1:1 ratio of sodium azide (0.032 g, 0.5 mmol) and potassium azide (0.040 g, 0.5 mmol). Slow evaporation of the resulting blue solutions produces well-formed crystals in 4-5 days in 50% yield. Anal. calculated/found (%) for **5**: C, 36.32/36.5; H 3.36/3.4; N 26.80/26.8.

Compound **6**: it was prepared following the same procedure than for complex **3** but changing the triethylamine by tetramethyl hydroxide (0.25 g, 1.5 mmol). In contrast with **3** that produces a large amount of well-formed crystals, complex **6** was obtained in a 40% yield of lower quality crystals. Anal. calculated/found (%) for **6**: C, 38.48/38.1; H 3.41/3.6; N 28.29/27.8. The same reaction employing NaN_3 as alkali cation source yielded a blue compound with a similar IR spectrum than **6** but its structure was not solved due to the poor quality of the crystals.

Compound **7**: to the common solution were added sodium methoxide (0.08 g, 1.5 mmol) and sodium azide (0.065 g, 1.0 mmol). Slow evaporation of the resulting solution gives well-formed crystals after one week in a 60% yield. Anal. calculated/found (%) for **7**: C, 45.13/45.8.2; H 3.41/3.2; N 24.20/23.9. The same reaction employing $Ca(OMe)_2$ as calcium cation source yielded a blue compound with a similar IR spectrum than **7** but its structure was not solved due to the poor quality of the crystals.

Acknowledgements

JM and AE thank the financial support from Ministerio de Economia y Competitividad, Project CTQ2018-094031-B-100. JM also acknowledges the support of a Juan de la Cierva Postdoctoral fellowship from the Spanish Ministerio de Ciencia Innovación y Universidades.

Keywords: nickel • metallamacrocycle • supramolecular • capsules • magnetism

References

[1] C. J. Brown, F. D. Toste, R. G. Bergman, K. N. Raymond, *Chem. Rev*. **2015**, *115*, 3012-3035.
[2] Y. Voloshin, I. Belaya, R. Krämer, The Encapsulation Phenomenon: Synthesis, Reactivity and Applications of Caged Ions and Molecules, Springer International Publishing, **2016**.
[3] K. Ariga, H. Ito, J. P. Hill, H. Tsukube, *Chem. Soc. Rev*. **2012**, *41*, 5800-5835
[4] T. L. Mako, J. M. Racicot, M. Levine, *Chem. Rev*. **2019**, *119*, 322-477.
[5] J. W. Steed, J. L. Atwood, Supramolecular Chemistry, (J. Wiley and Sons, **2009**).
[6] H. N. Motlagh, J. O. Wrabl, J. Li and V. J. Hilser, *Nature* **2014**, *508*, 331-339.
[7] C. M. A. Gangemi, A. Pappalardo, G. T. Sfrazzetto, *RSC Adv*. (review article) **2015**, *5*, 51919-51933.
[8] S. J. Dalgarno, N. P. Power, J. L. Atwood, *Coord. Chem. Rev*. **2008**, *252*, 825-841.
[9] H. Amouri, C. Desmarets, J. Moussa, *Chem. Rev*. **2012**, *112*, 2015-2041.
[10] F. J. Rizzuto, L. K. S. von Krbek, J. R. Nitschke, *Nature Rev. Chem*. **2019**, *3*, 204-222.
[11] T. C. Stamatatos, C. G. Efthymiou, C. C. Stoumpos, S. P. Perlepes, *Eur. J. Inorg. Chem*. **2009**, 3361-3391.
[12] Z. E. Serna, L. Lezama, M. K. Urtiaga, M. I. Arriortua, M. G. Barandika, R. Cortes, T. Rojo, *Angew. Chem. Int. Ed*. **2000**, *39*, 344-347.
[13] Z. Serna, N. De la Pinta, M. K. Urtiaga, L. Lezama, G. Madariaga, J. M. Clemente-Juan, E. Coronado, R. Cortes, *Inorg. Chem*. **2010**, *49*, 11541-11549.
[14] H.-S. Wang, Y. Song, *Inorg. Chem. Commun*. **2013**, *35*, 86-88.
[15] Z. E. Serna, M. G. Barandika, R. Cortes, M. K. Urtiaga, G. Barberis, T. Rojo, *J. Chem. Soc. Dalton Trans*. **2000**, 29-34.
[16] D.-Y. Wu, W. Huang, W.-J. Hua, Y. Song, C.-Y. Duan, S.-H. Li, Q.-J. Meng, *Dalton Trans*. **2007**, 1838-1845.
[17] A. K. Boudalis, M. Pissas, C. P. Raptopoulou, V. Psycharis, B. Abarca, R. Ballesteros, *Inorg. Chem*. **2008**, *47*, 10674-10681.
[18] G. S. Papaefstathiou, A. Escuer, R. Vicente, M. Font-Bardia, X. Solans, S. P. Perlepes, *Chem. Commun*. **2001**, 2414-2415.
[19] G. S. Papaefstathiou, A. K. Boudalis, T. C. Stamatatos, C. J. Milios, C. G. Efthymiou, C. P. Raptopoulou, A. Terzis, V. Psycharis, Y. Sanakis, R. Vicente, A. Escuer, J. P. Tuchagues, S. P. Perlepes, Polyhedron **2007**, *26*, 2089-2094.
[20] T. C. Stamatatos, C. P. Raptopoulou, S. P. Perlepes, A. K. Boudalis, Polyhedron **2011**, *30*, 3026-3033.
[21] A. N. Georgopoulou, C. P. Raptopoulou, V. Psycharis, R. Ballesteros, B. Abarca, A. K. Boudalis, *Inorg. Chem*. **2009**, *48*, 3167-3176.
[22] M.-L. Tong, M. Monfort, J. M. Clemente Juan, X.-M. Chen, X.-H. Bu, M. Ohba, S. Kitagawa, *Chem. Commun*. **2005**, 233-235.
[23] J. Mayans, M. Font-Bardia, A. Escuer, *Dalton Trans*. **2019**, 48, 16158-16561.
[24] A. Escuer, J. Esteban, S. P. Perlepes, T. C. Stamatatos, *Coord. Chem. Rev*. **2014**, *275*, 87-129.t
[25] T. T. Tran, J. Young, J. M. Rondinelli, P. S. Halasyamani, *J. Am. Chem. Soc*. **2017**, *139*, 1285-1295.
[26] A. Graham, S. Meier, S. Parsons, R. E. P. Winpenny, *Chem. Commun*. **2000**, 811-812.
[27] G. J. Cooper, G. N. Newton, P. Kogerler, D.-L. Long, L. Engelhardt, M. Luban, L. Cronin, *Angew. Chem. Int. Ed*. **2007**, *46*, 1340-1344.
[28] G. J. T.Cooper, G. N. Newton, D.-L. Long, P. Kogerler, M. H. Rosnes, M. Keller, L. Cronin, *Inorg. Chem*. **2009**, *48*, 1097-1104.
[29] A. Pons-Balague, S. Piligkos, S. J. Teat, J. S. Sanchez-Costa, M. Shiddiq, S. Hill, G. R. Castro, P. Ferrer-Escorihuela, E. Carolina Sañudo, *Chem. Eur. J*. **2013**, *19*, 9064-9071.
[30] P.-F. Yao, C.-H. Su, T.-X. Wu, You Li, H.-M. Hao, F.-P. Huang, Q. Yu, H.-D. Bian, *Polyhedron* **2018**, *141*, 37-43.
[31] G. Mezei, C. M. Zaleski, V. L. Pecoraro, Chem. Rev. **2007**, *107*, 4933-5003.
[32] J. Perez, L. Riera, (review) *Eur. J. Inorg. Chem*. **2009**, 4913–4925.
[33] D. Parasar, N. B. Jayaratna, A. Muñoz-Castro, A. E. Conway, P. K. Mykhailiuk, H. V. Rasika Dias, Dalton Trans. **2019**, *48*, 6358-6371.
[34] E. Ruiz, J. Cano, S. Alvarez, P. Alemany, *J. Am. Chem. Soc*., **1998**, *120*, 11122
[35] A. Escuer, R. Vicente, B. Mernari, A. El Gueddi, M. Pierrot, *Inorg. Chem*. **1997**, *36*, 2511-2516.
[36] K. Miyagi, Y. Kitagawa, M. Asaoka, R. Teramoto, Y. Natori, T. Saito, M. Nakano, *Polyhedron*, **2017**, *136*, 132-135.
[37] E. Escrivà , J. García-Lozano , J. Martínez-Lillo , H. Núñez , J. Server-Carrió , L. Soto , R. Carrasco, J. Cano, *Inorg. Chem*. **2003**, *42*, 8328-8336.
[38] Y. Elerman, E. Kavlakoglu, A. Elmali, *Z. Naturforsch* **2002**, *57a*, 919-924.
[39] A. Escuer, R. Vicente, E. Peñalba, X. Solans, Merce Font-Bardıa, *Inorg. Chem*. **1996**, *35*, 248-251;
[40] A. Escuer, R. Vicente, S. B. Kumar, X. Solans, Merce Font-Bardıa, A. Caneschi, *Inorg. Chem*. **1996**, *35*, 3094-3098.
[41] A. Escuer, E. Peñalba, R. Vicente, X. Solans, Mercé Font-Bardía, *J. Chem. Soc. Dalton Trans*. **1997**, 2315–2319.
[42] A. Escuer, R. Vicente, S. B. Kumar, F. A. Mautner, *J. Chem. Soc. Dalton Trans*. **1998**, 3473–3477.
[43] N. F. Chilton, R. P. Anderson, L. D. Turner, A. Soncini, K. S. Murray, *J. Comput. Chem*. **2013**, *34*, 1164-1165.
[44] G. M. Sheldrick, *Acta Crystallogr. Sect A: Fundam. Crystallogr*. **2008**, **64**, 112-122.
[45] L. J. Farrugia, *J. Appl. Crystallogr*. **1997**, *30*, 565.

FULL PAPER

Supramolecular {Ni_6-M_2-Ni_6} capsules and {Ni_6-M} bowls tailored by the ionic radius of the alkali cations and stabilized with Et_3NH^+ or Me_4N^+ co-cations have been built by assembly of {Ni_6} rings. Supramolecular interactions and magnetic response have been analyzed.

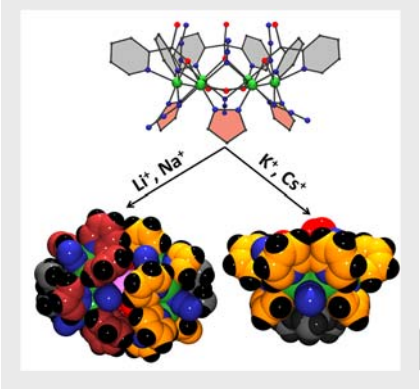

*Júlia Mayans, Constantinos C. Stoumpos, Mercé Font-Bardia and Albert Escuer**

Page No. – Page No.

From bowls to capsules: assembly of hexanuclear Ni^{II} rings tailored by alkali cations.